pp. 3 16 16

Sensor and Simulation Notes

Note 393

9 March 1996

Dielectric Body-of-Revolution Lenses with Azimuthal Propagation

Carl E. Baum
Phillips Laboratory

Abstract

This paper explores the design of dielectric lenses with nonuniform (but isotropic) permittivity and uniform permeability (such as μ_0). These lenses are exact in the sense that they propagate nondispersive TEM waves (and hence pulses) through a lens region which can be used to bend the direction of propagation through some angle of interest, here taken as the azimuthal angle ϕ appropriate to a portion of a body of revolution. Limitations associated with some of the boundaries of the lens region are pointed out. Four examples of this class of lenses are discussed.

1. Introduction

Searching for "exact" dielectric lenses, i.e., ones which support the propagation of dispersionless TEM waves which satisfy the Maxwell equations for all frequencies in the lens region, there are examples in [1, 2, 4]. By a dielectric lens, let us here mean one comprised of a scalar (isotropic) permittivity ε which is real and frequency independent (dispersionless) with $\varepsilon \geq \varepsilon_0$ (in the region of interest, the lens region), but which may be a function of position (i.e., inhomogeneous). Furthermore, the permeability μ is assumed real and frequency independent with $\mu \geq \mu_0$ as well as spatially independent (i.e., homogeneous). As a practical matter, one may often take $\mu = \mu_0$ (free-space permeability).

The general purpose of such a transient lens is to propagate transient EM waves with minimal pulse distortion while changing the direction of propagation (hence, transient lenses). Such might be a transition between two cylindrical transmission lines propagating waves in different directions, or one of these might be adjoined to a conical transmission line supporting a spherical TEM mode. Here let us restrict our attention to the very practical case of a purely dielectric lens, albeit inhomogeneous, so that it may need to be approximated by layers of dielectric material of various permittivities.

In the present paper we consider a class of such lenses as portions of a dielectric body of revolution (BOR) with propagation in the azimuthal (ϕ) direction. Such a lens is appropriate as a bending lens. As we shall see, there is an E-plane lens as in [1, 2], with circular cylindrical conducting boundaries, an H-plane lens as in [4] with planar conducting boundaries, and new examples with circular conical or spherical conducting boundaries.

2. Body-of-Revolution Coordinates

Begin with Cartesian coordinates (x, y, z) on which we base the usual cylindrical coordinates (Ψ, ϕ, z) with

$$x = \Psi\cos(\phi) \quad , \quad y = \Psi\sin(\phi) \tag{2.1}$$

and spherical coordinates (r, θ, ϕ) with

$$\begin{aligned} z &= \Psi\cos(\theta) \quad , \quad \Psi = r\sin(\theta) \\ x &= r\sin(\theta)\cos(\phi) \quad , \quad y = r\sin(\theta)\sin(\phi) \end{aligned} \tag{2.2}$$

The dielectric BOR is defined to have the z axis as the symmetry axis. This is $C_{\infty a}$ symmetry indicating invariance to rotation (variation of ϕ) with all axial planes (containing the z axis) as symmetry planes (noting that ε is scalar, besides being ϕ independent) [5].

For our BOR, let us define an orthogonal curvilinear coordinate system (ξ_1 , ξ_2 , ξ_3) where we choose

$$\xi_3 \equiv \phi \equiv \text{propagation coordinate} \tag{2.3}$$

and ξ_1 and ξ_2 will be used for orientations of the electric and magnetic fields. Surfaces of constant ξ_3 are planes and surfaces of constant ξ_1 as well as surfaces of constant ξ_2 are BORs. Of course all three types of surfaces intersect at right angles (except at possible singularities). Cylindrical and spherical coordinates (above) are examples of such orthogonal curvilinear systems. Later, similar to the technique in [2], we will use (u_1 , u_2 , u_3) orthogonal curvilinear coordinates where each u_n is only a function of ξ_n. Constant ξ_n surfaces are then also constant u_n surfaces.

Considering a plane of constant ξ_3, then ξ_1 and ξ_2 are orthogonal curvilinear coordinates on this surface. Then one can base the ξ_1 and ξ_2 coordinates on a conformal transformation involving the complex variables

$$\begin{aligned} \zeta &\equiv \xi_1 \pm j\xi_2 \\ \zeta &\equiv z + j\Psi \\ \xi(\zeta) &\equiv \text{analytic function} \equiv \text{conformal transformation} \end{aligned} \tag{2.4}$$

(See [4 (Appendix A.5)].)

Consider next one of the BOR surfaces, say one specified by constant ξ_1. Then ξ_2 and ξ_3 are orthogonal curvilinear coordinates on this surface. Such surfaces have important properties as discussed in [3 (Section 46)]. Lines of constant ξ_3 are plane curves (i.e., lie in a plane of constant ξ_3) and are called *meridians*. (On a sphere, these are lines of longitude.) Lines of constant ξ_2 are circles (and hence plane curves lying in planes of constant z) and are called *parallels*. (On a sphere, these are lines of latitude.) One can also base the ξ_2 and ξ_3 coordinates on a conformal transformation as before. The other set of BOR surfaces, specified by constant ξ_2, have all the same properties, with now lines of constant ξ_3 still the meridians, but lines of constant ξ_1 as the parallels.

Given some initial choice of the ξ_n, we will scale them as $u_n(\xi_n)$. For this purpose, we will need the scale factors

$$h_n^2 = \left(\frac{\partial x}{\partial u_n}\right)^2 + \left(\frac{\partial y}{\partial u_n}\right)^2 + \left(\frac{\partial z}{\partial u_n}\right)^2 \tag{2.5}$$

which give the line element

$$(d\ell)^2 = \sum_{n=1}^{3} h_n^2 (du_n)^2 \tag{2.6}$$

Noting that u_3 is a function of only ϕ we have

$$h_\phi = \Psi = r\sin(\theta) \quad , \quad h_3 = \Psi \left|\frac{d\phi}{du_3}\right| \tag{2.7}$$

3. Electromagnetic Plane Waves Propagating in the ϕ Direction

Consider a homogeneous TEM wave as expressed in terms of the formal fields with the form [4 (Section 2.5)]

$$\begin{aligned} E_1' &= h_1 E_1 = E_o' f\left(t - \frac{u_3}{c'}\right) \\ H_2' &= h_2 H_2 = \frac{E_o'}{Z_o'} f\left(t - \frac{u_3}{c'}\right) \end{aligned} \tag{3.1}$$

where these are the only two non-zero field components. This is an important restriction in that it gives us more flexibility in the selection of our coordinate systems than in the case of inhomogeneous TEM waves (1 and 2 components for both electric and magnetic fields [4 (Section 2.4)]).

For diagonal $\overleftrightarrow{\varepsilon}$ and $\overleftrightarrow{\mu}$, the formal constitutive parameters are related to the usual ones via

$$\begin{aligned} \overleftrightarrow{\varepsilon}' &= \left(\gamma_{n,m}\right) \cdot \overleftrightarrow{\varepsilon} \quad , \quad \overleftrightarrow{\mu}' = \left(\gamma_{n,m}\right) \cdot \overleftrightarrow{\mu} \\ \left(\gamma_{n,m}\right) &= \begin{pmatrix} \frac{h_2 h_3}{h_1} & 0 & 0 \\ 0 & \frac{h_3 h_1}{h_2} & 0 \\ 0 & 0 & \frac{h_1 h_2}{h_3} \end{pmatrix} \end{aligned} \tag{3.2}$$

Since we only have E_1 and H_2 components to consider, this reduces to

$$\varepsilon' = \frac{h_2 h_3}{h_1} \varepsilon \quad , \quad \mu' = \frac{h_3 h_1}{h_2} \mu \tag{3.3}$$

Since we are assuming that μ is homogeneous we have, for convenience

$$\begin{aligned} \mu &= \mu' \geq \mu_o \quad , \quad \frac{h_3 h_1}{h_2} = 1 \\ \varepsilon &= \frac{h_1}{h_2 h_3} \varepsilon' = h_3^{-2} \varepsilon' \quad , \quad \varepsilon' \geq \varepsilon_o \end{aligned} \tag{3.4}$$

noting that both μ' and ε' are real and frequency independent by hypothesis.

The propagation speeds are

$$c' = [\mu' \varepsilon']^{-\frac{1}{2}} \quad , \quad c_w = [\mu \varepsilon]^{-\frac{1}{2}} = h_3 \; c' = \text{local wave speed} \tag{3.5}$$

Noting that ε and hence c_w is independent of ϕ we have u_3 proportional to ϕ as

$$u_3 = \Psi_{max}\phi \quad , \quad h_3 = \frac{\Psi}{\Psi_{max}} = \frac{h_2}{h_1} \tag{3.6}$$

where Ψ_{max} is the largest Ψ of interest for the lens region. Then we have

$$\begin{aligned} \varepsilon &= \left(\frac{\Psi_{max}}{\Psi}\right)^2 \varepsilon_{min} \quad , \quad \varepsilon_{min} = \varepsilon' \\ c_w &= \frac{\Psi}{\Psi_{max}} \; c' \le c' \le c \text{ for } \Psi \le \Psi_{max} \end{aligned} \tag{3.7}$$

So Ψ_{max} is an important parameter where $\varepsilon = \varepsilon_{min}$ and c_w is at its maximum so as to meet realizability conditions in the lens region. Note also that the local wave impedance is

$$\begin{aligned} Z_w &= \frac{E_1}{H_2} = \frac{h_2}{h_1} \; Z_o' = h_3 \; Z_o' = \frac{\Psi}{\Psi_{max}} Z_o' \\ Z_o' &= \left[\frac{\mu'}{\varepsilon'}\right]^{\frac{1}{2}} = \left[\frac{\mu}{\varepsilon_{min}}\right]^{\frac{1}{2}} \equiv \text{formal wave impedance} \end{aligned} \tag{3.8}$$

and Z_w is minimum at $\Psi = \Psi_{max}$. The above parameters apply to all the examples which follow. Note in particular that h_2 / h_1 is Ψ / Ψ_{max} for all these examples; we need to find factored forms for h_2 / h_1 so that u_1 and u_2 are mutually orthogonal coordinates to construct such examples.

The above results concern only the u_3 coordinate and the implications that the lens is part of a BOR. This is enough to specify ε and a range of acceptable cylindrical radius Ψ. This leaves our choice of u_1 and u_2 to give various lens geometries. While this is not critical to the discussion we can regard the lens region as limited to

$$\phi_1 \le \phi \le \phi_2 \quad , \quad 0 < \phi_2 - \phi_1 < 2\pi \tag{3.9}$$

While our examples have boundaries which may be functions of z and Ψ, these boundaries are in turn contained in regions limited by

$$0 < \Psi \leq \Psi_{max} \quad , \quad z_1 \leq z \leq z_2 \quad , \quad z_1 < z_2 \tag{3.10}$$

A general result that applies to homogeneous formal TEM waves as in (3.1) concerns transmission-line characteristic impedance Z_c. If we have a lens region given by

$$\begin{aligned} u_1^{(1)} \leq u_1 \leq u_1^{(2)} \quad , \quad u_2^{(1)} \leq u_2 \leq u_2^{(2)} \\ u_1^{(1)}, u_1^{(2)} \equiv \text{electric boundaries} \\ u_2^{(1)}, u_2^{(2)} \equiv \text{magnetic boundaries} \end{aligned} \tag{3.11}$$

then the TEM wave can be considered as a TEM mode on a transmission line with characteristic impedance

$$\begin{aligned} Z_c = \frac{V}{I} &\equiv \frac{\int_{u_1^{(1)}}^{u_1^{(2)}} E_1 \, h_1 \, du_1}{\int_{u_2^{(1)}}^{u_2^{(2)}} H_2 \, h_2 \, du_2} = \frac{\int_{u_1^{(1)}}^{u_1^{(2)}} E_1' \, du_1}{\int_{u_2^{(1)}}^{u_2^{(2)}} H_2' \, du_2} \\ &= Z_o' \, \frac{u_1^{(2)} - u_1^{(1)}}{u_2^{(2)} - u_2^{(1)}} \equiv Z_o' \, \frac{\Delta u_1}{\Delta u_2} \end{aligned} \tag{3.12}$$

Note that the line element for the integration of the fields along each u_n is $h_n \, u_n$ as in (2.6).

The electric boundaries can be realized by approximately perfectly conducting sheets. If the u_2 coordinate encircles a conductor so that Δu_2 represents the change in u_2 around the conductor, then the field continuity through the common surface defined by both $u_2^{(1)}$ and $u_2^{(2)}$ satisfies the properties required of a magnetic boundary. (This gives a jacket as in [4 (Chapter 5)].) If we have

$$0 < \Delta u_1 << \Delta u_2 \tag{3.13}$$

so that Z_c is a low impedance, then we can have the case that magnetic-field lines do not close in the lens region with $u_2^{(1)}$ and $u_2^{(2)}$ as distinct surfaces. Then the energy in the fringe fields (by definition outside the lens region) is small compared to the energy in the lens region, and can be neglected in a limiting sense. Such is the case for closely spaced conducting sheets (compared to their width) as in a strip line. The later examples will have to be considered with this in mind.

4. Examples Based on Cylindrical Coordinates

Let us first cast two previous solutions based on cylindrical coordinates in the present format.

4.1 H-Plane Bend

In [4 (Appendix F)] the case of constant μ corresponds to an H-Plane bend with perfectly conducting boundaries on planes of constant z, say z_1 and z_2, as illustrated in fig. 4.1. Putting this in the context of our present cylindrical coordinates for a BOR lens gives

$$\begin{aligned}
&\vec{E} = E_1 \vec{1}_z \ , \ \vec{H} = H_2 \vec{1}_\Psi \ , \ \vec{1}_1 = \vec{1}_z \ , \ \vec{1}_2 = \vec{1}_\Psi \\
&u_1 = z \ , \ h_1 = 1 \\
&u_2 = u_2(\Psi) \\
&h_2 = \left|\frac{d\Psi}{du_2}\right| = h_1 h_3 = \frac{\Psi}{\Psi_{max}} \\
&u_2 = \Psi_{max} \, \ell n\left(\frac{\Psi}{\Psi_{max}}\right)
\end{aligned} \tag{4.1}$$

where the integration constants have been chosen for convenience with the constraint that the u_n form a right-handed system. The fields then take the form

$$\begin{aligned}
E_1 &= \frac{E_1'}{h_1} = E_o' \, f\left(t - \frac{u_3}{c'}\right) \\
H_2 &= \frac{H_2'}{h_2} = \frac{\Psi_{max}}{\Psi} \, \frac{E_o'}{Z_o'} \, f\left(t - \frac{u_3}{c'}\right)
\end{aligned} \tag{4.2}$$

Note that E_1 is uniform with respect to z and Ψ while H_2 varies as Ψ^{-1}.

The lens domain is limited as

$$\begin{aligned}
&0 < \Psi_1 \le \Psi \le \Psi_2 \le \Psi_{max} \\
&\phi_1 \le \phi \le \phi_2 \ , \ z_1 \le z \le z_2
\end{aligned} \tag{4.3}$$

While z_1 and z_2 are realizable as approximately perfectly conducting boundaries, Ψ_1 and Ψ_2 are ideally magnetic boundaries which are difficult to realize. As a practical matter, one can choose

$$z_2 - z_1 << \Psi_2 - \Psi_1 \tag{4.4}$$

to give a low-impedance configuration in which the effect of the fringe fields can be reduced.

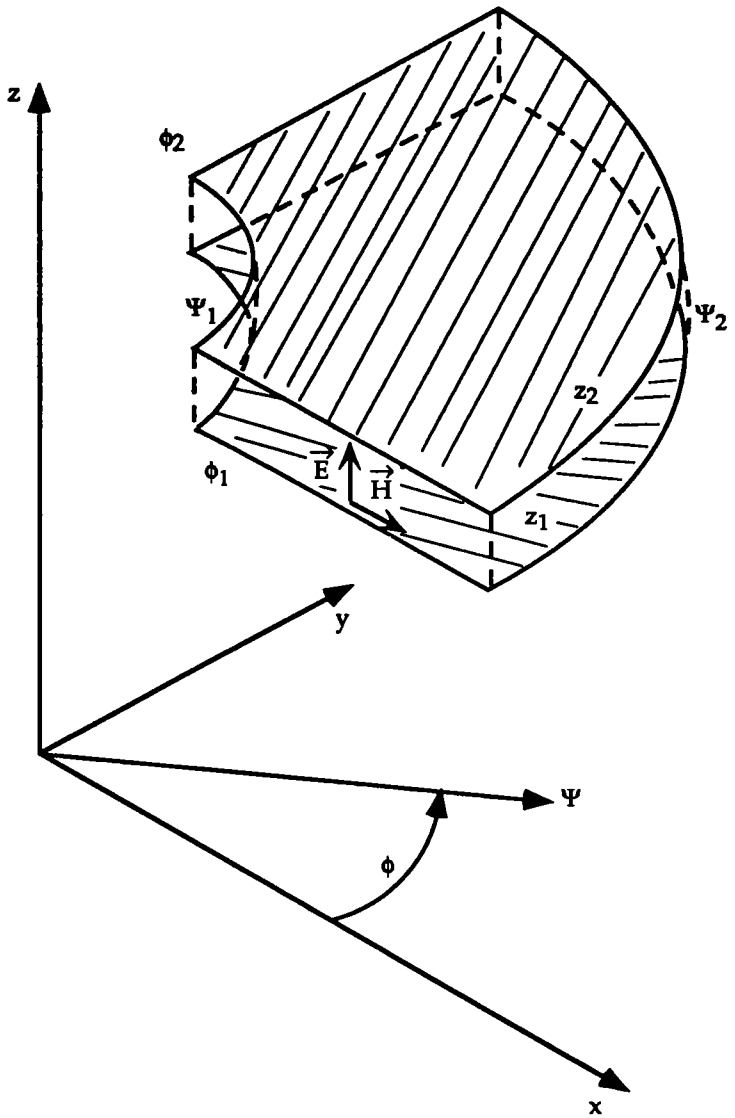

Fig. 4.1. H-Plane Bend

4.2 E-Plane Bend

In [2] we have the case of an E-plane bend with perfectly conducting boundaries on circular cylinders of constant Ψ, say Ψ_1 and Ψ_2, as illustrated in fig. 4.2. In our present context, this gives

$$\begin{aligned}
&\vec{E} = -E_1 \vec{1}_\Psi \quad , \quad \vec{H} = H_2 \vec{1}_z \quad , \quad \vec{1}_1 = -\vec{1}_\Psi \quad , \quad \vec{1}_2 = \vec{1}_z \\
&u_2 = z \quad , \quad h_2 = 1 \\
&u_1 = u_1(\Psi) \\
&h_1 = \left|\frac{d\Psi}{du_1}\right| = \frac{h_2}{h_3} = \frac{\Psi_{max}}{\Psi} \\
&u_1 = -\frac{\Psi^2}{2\Psi_{max}}
\end{aligned} \tag{4.5}$$

Again, the integration constants are chosen for convenience with the u_n forming a right-handed system. The fields then take the form

$$\begin{aligned}
E_1 &= \frac{E_1'}{h_1} = \frac{\Psi}{\Psi_{max}} E_0' f\left(t - \frac{u_3}{c'}\right) \\
H_2 &= \frac{H_2'}{h_2} = \frac{E_0'}{Z_0'} f\left(t - \frac{u_3}{c'}\right)
\end{aligned} \tag{4.6}$$

In this case H_2 is uniform with respect to z and Ψ while E_1 varies as Ψ (maximum at the *outer* boundary Ψ_2).

The lens domain is limited as

$$\begin{aligned}
&0 < \Psi_1 \le \Psi \le \Psi_2 \le \Psi_{max} \\
&\phi_1 \le \phi \le \phi_2 \quad , \quad z_1 \le z \le z_2
\end{aligned}\ \text{s} \tag{4.7}$$

While Ψ_1 and Ψ_2 are realizable as approximately perfectly conducting boundaries, z_1 and z_2 are ideally magnetic boundaries. Choosing

$$\Psi_2 - \Psi_1 \le z_2 - z_1 \tag{4.8}$$

gives a low-impedance configuration which minimizes the effect of fringe fields.

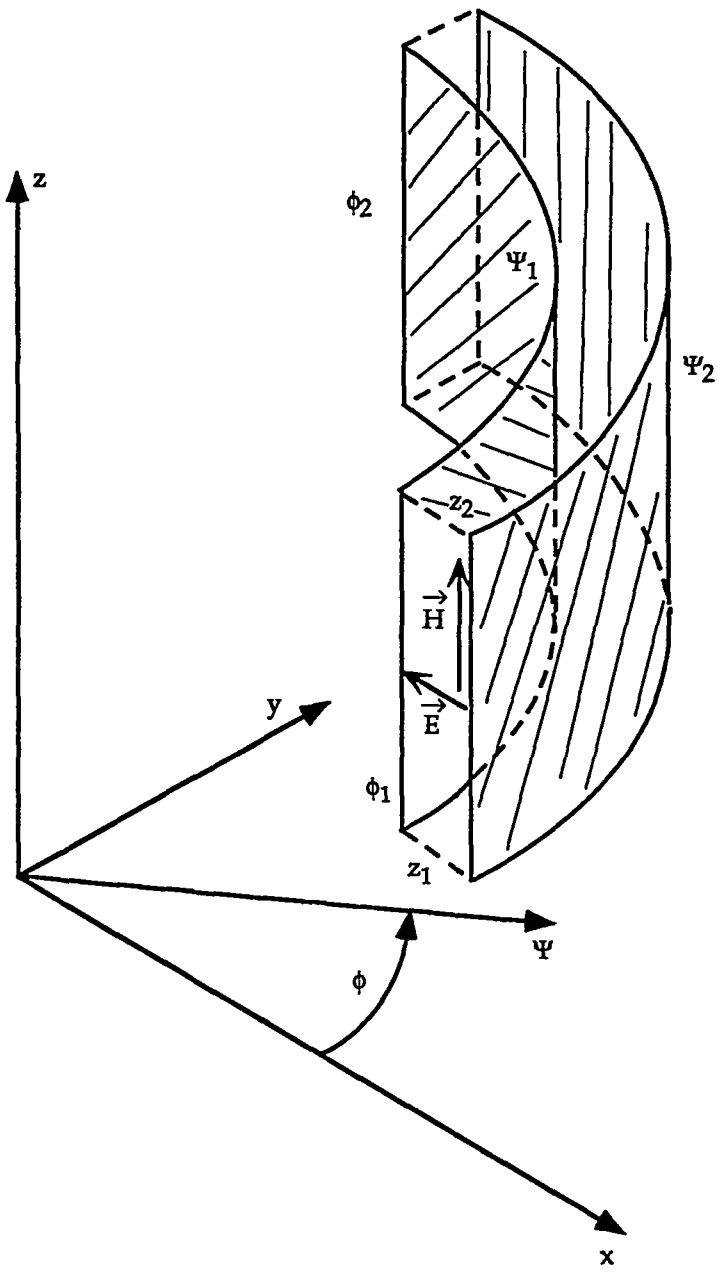

Fig. 4.2. E-Plane Bend

5. Examples Based on Spherical Coordinates

Now let us exhibit two new solutions based on spherical coordinates. These are neither E- nor H-plane bends but might be referred to as mixed bends. Boundaries are circular-conical and spherical surface segments. The two cases are based on letting u_1 and u_2 each be functions of r or θ alone in some order.

5.1 Circular Conical Conducting Boundaries

For this case refer to fig. 5.1 with the choices of field orientations

$$\begin{aligned} &\vec{E} = -E_1\ \vec{1}_\theta\ ,\ \vec{H} = H_2\ \vec{1}_r\ ,\ \vec{1}_1 = -\vec{1}_\theta\ ,\ \vec{1}_2 = \vec{1}_r \\ &u_1 = u_1(\theta)\ ,\ u_2 = u_2(r) \end{aligned} \tag{5.1}$$

From

$$\frac{h_2}{h_1} = \frac{\Psi}{\Psi_{max}} = \frac{r\ \sin(\theta)}{\Psi_{max}} \equiv \frac{r\sin(\theta)}{r_{max}\sin(\theta_{max})}$$

and noting that the line element in the θ direction is $rd\theta$ (i.e., $h_\theta = r$) we can select

$$\begin{aligned} h_1 &= \left|\frac{rd\theta}{du_1}\right| = \frac{r}{r_{max}}\ \frac{\sin(\theta_{max})}{\sin(\theta)} \\ h_2 &= \left|\frac{dr}{du_2}\right| = \left(\frac{r}{r_{max}}\right)^2 \end{aligned} \tag{5.2}$$

This allows u_1 and u_2 to be solved as

$$\begin{aligned} u_1 &= r_{max}\ \frac{\cos(\theta)}{\sin(\theta_{max})} \\ u_2 &= -\frac{r_{max}^2}{r} \end{aligned} \tag{5.3}$$

where the integration constants have been chosen for convenience. The fields then take the form

$$\begin{aligned} E_1 &= \frac{E_1'}{h_1} = \frac{r_{max}}{r}\ \frac{\sin(\theta)}{\sin(\theta_{max})} E_0'\ f\left(t - \frac{u_3}{c'}\right) \\ H_2 &= \frac{H_2'}{h_2} = \left(\frac{r_{max}}{r}\right)^2\ \frac{E_0'}{Z_0'} f\left(t - \frac{u_3}{c'}\right) \end{aligned} \tag{5.4}$$

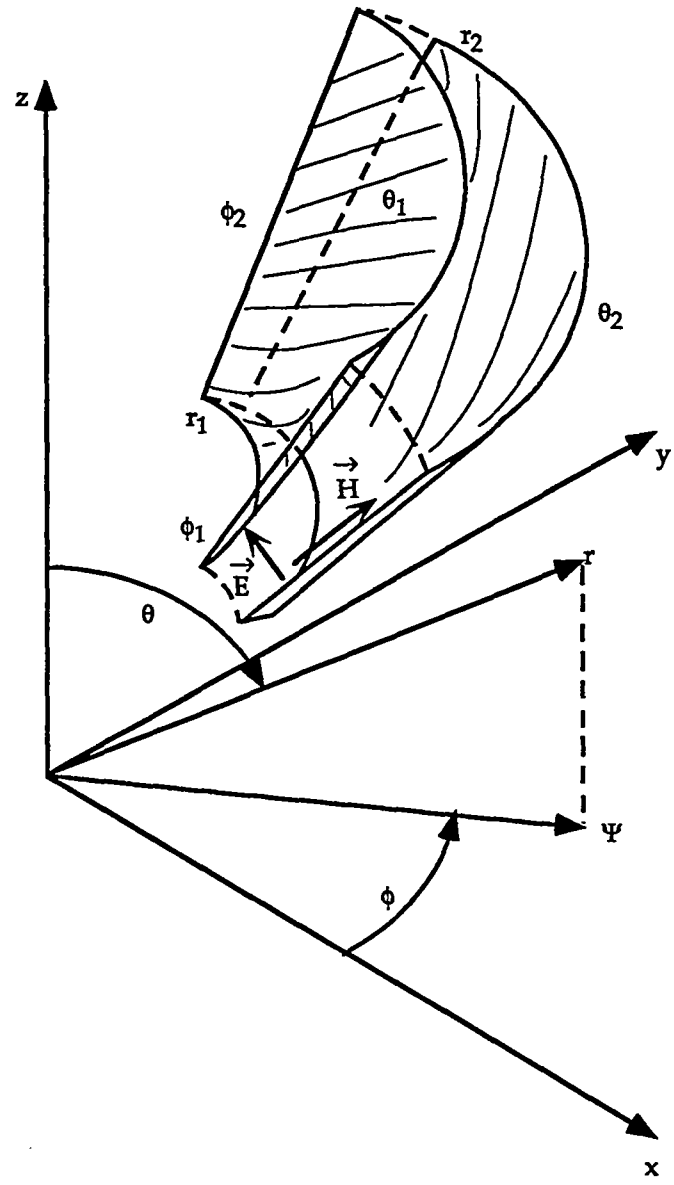

Fig. 5.1. Mixed Bend with Circular Conical Conducting Boundaries

The lens domain is limited as

$$0 < r_1 \le r \le r_2 \le r_{max}$$
$$\phi_1 \le \phi \le \phi_2 \ , \ 0 < \theta_1 \le \theta \le \theta_2 \le \theta_{max} \tag{5.5}$$

Now θ_1 and θ_2 are the electric boundaries, while the magnetic boundaries are given by r_1 and r_2. In line with previous considerations one can choose

$$r_2 [\theta_2 - \theta_1] << r_2 - r_1 \tag{5.6}$$

to give a low-impedance configuration and small fringe-field effects.

One might think that this solution of the Maxwell equations has a strange form. The electric field is proportional to r^{-1} consistent with the increasing conductor spacing for larger r , and to $\sin(\theta)$ due to the decreasing ε for larger Ψ (and hence θ). The magnetic field is proportional to r^{-2}. One factor of r^{-1} accounts for the increasing conductor spacing with larger r^{-1}; the second factor of r^{-1} accounts for spreading of the magnetic flux proportional to $rd\phi$ in some incremental $d\phi$ along the direction of propagation (normal to $\vec{H}$). This is necessary to give zero divergence to $\vec{H}$ which is like the r^{-2} field from a magnetic monopole at $\vec{r} = \vec{0}$, except for the variation in the ϕ (propagation) direction (i.e., transit time or phase).

5.2 Spherical Conducting Boundaries

For this case, refer to fig. 5.2 with the choices of field orientations

$$\vec{E} = E_1 \vec{1}_r \ , \ \vec{H} = H_2 \vec{1}_\theta \ , \ \vec{1}_1 = -\vec{1}_r \ , \ \vec{1}_2 = \vec{1}_\theta$$
$$u_1 = u_1(r) \ , \ u_2 = u_2(\theta) \tag{5.7}$$

From

$$\frac{h_2}{h_1} = \frac{\Psi}{\Psi_{max}} = \frac{r \sin(\theta)}{\Psi_{max}} \equiv \frac{r \sin(\theta)}{r_{max} \sin(\theta_{max})} \tag{5.8}$$

with the line element as $rd\theta$ in the θ direction we can select

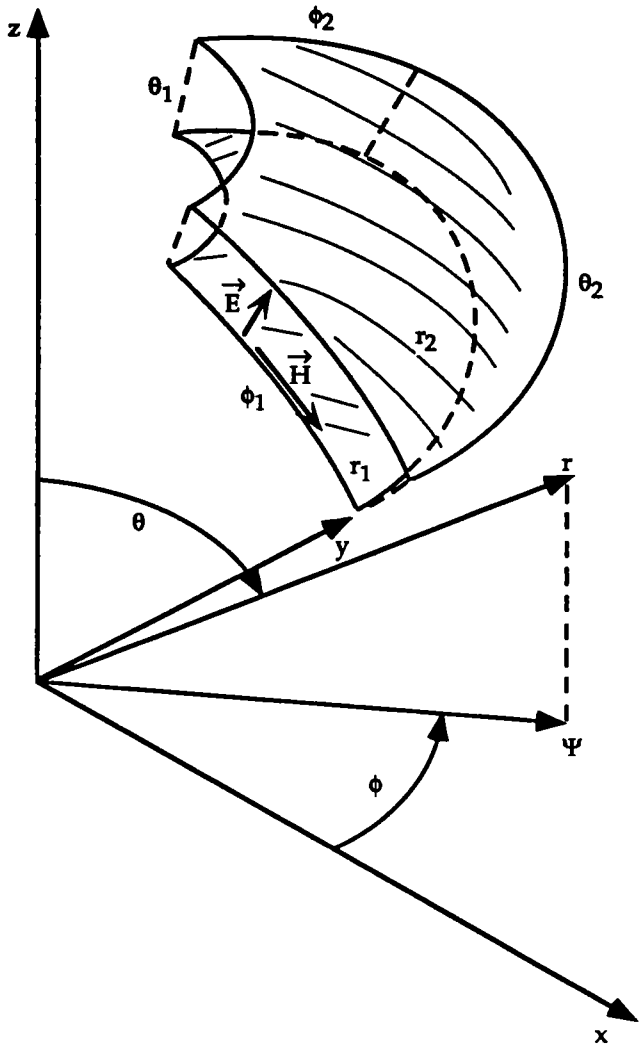

Fig. 5.2. Mixed Bend with Spherical Conducting Boundaries

$$h_2 = \left|\frac{r d\theta}{du_1}\right| = \frac{r \sin(\theta)}{r_{max} \sin(\theta_{max})}$$
$$h_1 = \left|\frac{dr}{du_2}\right| = 1 \qquad (5.9)$$

This allows u1 and u2 to be solved as

$$u_1 = r$$
$$u_2 = r_{max} \sin(\theta_{max}) \, \ell n \left[\frac{\tan\left(\frac{\theta}{2}\right)}{\tan\left(\frac{\theta_{max}}{2}\right)}\right] \qquad (5.10)$$

where the integration constants have been chosen for convenience. The fields then take the form

$$E_1 = \frac{E_1'}{h_1} = E_o' f\left(t - \frac{u_3}{c'}\right)$$
$$H_2 = \frac{H_1'}{h_2} = \frac{r_{max}}{r} \frac{\sin(\theta_{max})}{\sin(\theta)} \frac{E_o'}{Z_o'} f\left(t - \frac{u_3}{c'}\right) \qquad (5.11)$$
$$= \frac{\Psi_{max}}{\Psi} \frac{E_o'}{Z_o'} f\left(t - \frac{u_3}{c'}\right)$$

6. Concluding Remarks

We have here four types of "exact" dielectric lenses for bending the direction of propagation along the azimuthal coordinate of a BOR. All have the same dependence of the permittivity as proportional to Ψ^{-2}. The difference in the various lens types lies in the choice of coordinates on a meridian plane. Noting that there are two choices for polarization, the Cartesian (z, Ψ) and polar (r, θ) coordinates produce the four examples. This gives some flexibility in the lens design for a given angle of bend $\phi_2 - \phi_1$ desired.

While the Maxwell equations are satisfied for a TEM wave in the lens region, there are the boundaries to consider. The electric boundaries can be well approximated by metal sheets. As discussed previously, the magnetic boundaries are more problematical, but the effect of the fringe fields there can be reduced by using low-impedance lenses. There is also the problem of matching the wave to other waveguiding structures at ϕ_1 and ϕ_2 where some perturbation of the TEM mode may occur.

Noting that all of these examples have the same form of the permittivity $\varepsilon(\Psi)$, one can consider linear combinations of these TEM waves as also solutions of the Maxwell equations. Keeping the waveform $f(t - u_3 / c')$ the same in all cases then one can look at the orientation of the electric and magnetic fields to determine the contours (in the Ψ, z or r, θ plane) for the appropriate boundaries for the TEM waveguide. Also noting that the coordinate origin can be taken anywhere along the z axis, then the spherical-coordinate solutions exist for any such choice of $\vec{r} = 0$, giving in effect an infinite number of spherical cases, two for each choice of coordinate origin. Thus the present cases (canonical solutions) can lead to various other lens designs.

Here the discussion has been for constant μ, but variable ε. The dual problem has constant ε, but variable μ, with the roles of electric and magnetic fields interchanged (as well as electric and magnetic boundaries interchanged). So the present examples can all be used to generate a dual set of examples with the appropriate interchange of parameters in the equations.

References

1. C. E. Baum, Wedge Dielectric Lenses for TEM Waves Between Parallel Plates, Sensor and Simulation Note 332, September 1991.

2. C. E. Baum, Two-Dimensional Inhomogeneous Dielectric Lenses for E-Plane Bends of TEM Waves Guided Between Perfectly Conducting Sheets, Sensor and Simulation Note 388, October 1955.

3. L. P. Eisenhard, *A Treatise on the Differential Geometry of Curves and Surfaces*, Dover, 1960.

4. C. E. Baum and A. P. Stone, *Transient Lens Synthesis: Differential Geometry in Electromagnetic Theory*, Hemisphere (Taylor & Francis), 1991.

5. C. E. Baum and H. N. Kritikos, Symmetry in Electromagnetics, ch. 1, pp. 1-90, in C. E. Baum and H. N. Kritikos (eds.), *Electromagnetic Symmetry*, Taylor & Francis, 1995.